Evolution of deformation in the neutron-rich Zr region from excited intruder state to the ground state

G. Lhersonneau,* B. Pfeiffer, and K.-L. Kratz
Institut für Kernchemie, Universität Mainz, D-55099 Mainz, Germany

T. Enqvist, P. P. Jauho, A. Jokinen, J. Kantele,† M. Leino,
J. M. Parmonen, H. Penttilä, and J. Äystö
Department of Physics, University of Jyväskylä, P.B. 35, FIN-40351 Jyväskylä, Finland

and the ISOLDE Collaboration
CERN, CH-1211 Genève 23, Switzerland
(Received 20 August 1993)

Strong evidence for the existence of previously postulated deformed excited states in $^{98}Zr_{58}$ has been obtained by an accurate measurement of the $\rho^2(0_3^+ \rightarrow 0_2^+)$ value for the decay of the second excited 0^+ state at 1436 keV. In the neighboring isotope $^{99}Zr_{59}$, at the edge of the region of strong ground-state deformation, evidence is found for a rotational band built on the state at 614 keV. Systematics of the excitation energies of the deformed states in Zr nuclei and their Sr neighbors show that the apparent sudden onset of deformation is explained by the steady lowering of a strongly deformed potential minimum. Therefore, an extra strong interaction between proton-neutron spin-orbit partners, acting in the 0_2^+ states, need not be invoked to explain the origin of the sudden onset of deformation.

PACS number(s): 27.60.+j, 23.20.Lv, 21.10.Re

I. INTRODUCTION

The neutron-rich isotopes of $_{38}Sr$, $_{39}Y$, and $_{40}Zr$ exhibit a unique sudden change of ground-state shapes from $N \leq 59$ to $N = 60$. The isotopes near $^{96}Zr_{56}$ show very little collectivity, which was first evidenced by the high 2^+ energies of 1751 and 1223 keV in ^{96}Zr and ^{98}Zr, respectively. In the Sr isotopes, the first 2^+ states lie around 800 keV, which could be an indication of a more vibrational structure. However, recent lifetime measurements of these levels at TRISTAN [1] have demonstrated that the $E2$ rates are only slightly enhanced. The data available for the odd-neutron Sr and Zr and for the odd-proton Y isotopes fully support a spherical character for the low-lying states of these nuclei with $N \leq 59$. The first hint for the existence of deformed states came from a study of the $A = 98$ chain at OSTIS [2]. The authors reported $E0$ transitions in ^{98}Zr with large ρ^2 values, which could indicate the presence of deformation. One of the goals of the present study was to obtain more detailed information on the existence and strength of the $E0$ transitions among the high-lying levels in ^{98}Zr. The interpretation of the data was expected to be facilitated by new and more accurate lifetime measurements of the 0^+ states [3].

While nuclei with $N \geq 60$ have strong ground-state deformations with the quadrupole deformation parameter β about 0.40 as given in Refs. [4,5] for Sr, in Ref. [6] for Y, and in Refs. [7,8] for Zr, the intermediate $N = 59$ isotones ^{97}Sr [9] and ^{98}Y [10] still appear to have spherical ground states. However, they show shape coexistence with deformed states appearing at about 500 keV excitation. Lifetimes of the first members of some of these excited bands have been measured for ^{97}Sr [11] and ^{98}Y [12], suggesting deformations almost as strong as those observed for their more neutron-rich neighboring isotopes. The data for ^{99}Zr [13] indicate a structure similar to that of ^{97}Sr at low energy, but still do not show clearly the existence of deformed excited states, as one expects from systematics. Therefore, a more detailed knowledge of the level scheme of ^{99}Zr is necessary in order to possibly find fingerprints of deformation. Thus, the present investigation aims at establishing the existence of deformed excited states as intruders in the region of spherical ground states with $N = 58,59$.

II. EXPERIMENTAL METHODS

A. Experiments at IGISOL

The yttrium isotopes, β-decay parents of Zr, were produced mainly as primary beams at the IGISOL facility using proton-induced fission following the bombardment of four 20 mg/cm^2 thick ^{238}U targets with 20 MeV proton energy [14]. The most probable nuclear charge of the fission products for $A = 98$ and 99 can be estimated to be about 39.0 and 39.5, respectively [15]. The half

*Now at Physics Department, University of Jyväskylä.
†Deceased.

widths of these charge distributions are of the order of one charge unit or less. This means that most of the direct production for $A = 98$ and 99 concentrates on strontium, yttrium and zirconium. Short-lived radioactive beams of these elements are well produced with the ion-guide technique with a delay time as short as 1 ms. This property and the direct population in fission allow the detection of the decays of low as well as high-spin states and provide complementary information to studies at OSTIS and ISOLDE, where only low-spin states of Y and Zr isotopes are available as β-decay products. A drawback of the IGISOL technique is that, due to the relatively low pressure of helium (100 mbar) used to thermalize energetic fragments the efficiency is only of the order of 10^{-3}. However, the production rates of mass separated ^{98}Y and ^{99}Y were a few hundred atoms/μC, which is quite adequate for spectroscopic studies.

Radioactive beams of interest were implanted on a collector tape, which could be moved to remove the built-up long-lived background activities at the implantation and detection position. The tape was moved every 6 s and every 600 s for $A = 98$ and 99, respectively. The radioactive decay of the mass-separated source on the tape was measured using the electron-transporter spectrometer ELLI [16] and the close-geometry 1.4 cm^3 GeHP detector both in singles and coincidence modes including fast timing. The events consisting of the electron energy, γ-ray energy, time between the detectors, as well as the time of occurrence of the event, were stored in the list mode on magnetic tape.

Energy and efficiency calibrations for γ rays were done by placing standard sources at the collection point. This procedure improved the efficiency calibration at low energy, which in the experiments at OSTIS and ISOLDE was determined internally using only a limited number of calibration points. The calibration procedure and the efficiency of ELLI are described in Ref. [16]. The efficiency in the on-line mode was about 16% at 100 keV and about 6% at 500 keV. The efficiency curve was checked during the experiment using known transitions in nuclei belonging to the mass numbers studied. The relative error of the efficiency was estimated to be 15%.

B. Experiment on ^{99}Zr at OSTIS and ISOLDE

The bulk of the data originates from an experiment at the OSTIS separator at ILL-Grenoble. The isotope ^{99}Zr was populated in the β decay of ^{99}Y, which itself is a decay product of mass-separated ^{99}Rb and ^{99}Sr. Singles γ and γ-γ-t coincidences were recorded with two medium-size Ge(Li) detectors covering a range from 10 keV (singles) and 25 keV (coincidences) up to 2000 keV. The time window was about 1 μs. The duration of the experiment was about 2 weeks. Some of the results of this experiment, concerning the level schemes of ^{99}Sr and ^{99}Y, have been reported earlier [17]. In addition, singles spectra for the high-energy range up to 4 MeV were recorded at the ISOLDE separator with a large volume Ge detector. There, the ^{99}Y parent nucleus was a product of the β-delayed neutron decay of mass separated ^{100}Rb [5].

III. EXPERIMENTAL RESULTS

A. 0^+ states in ^{98}Zr

The singles spectra in Fig. 1 show electron transitions at 405.0(2) and 564.0(2) keV, in agreement with the previous findings of 405.4 and 564.3 keV [2]. The electron lines were seen in a projection gated by the $K\alpha$ Zr line. At the corresponding γ energies of 423.0 and 582.0 keV no peaks could be seen, implying that the multipolarity of the transitions is at least $M3$. It is very unlikely to find such transitions in the even-even nucleus ^{98}Zr. Thus, in agreement with [2], the transitions must have $E0$ multipolarity. Moreover, the sum of their energies fits very well the difference of the excitation energies of the 0_4^+ to 0_2^+ levels as given in Ref. [18]. The partial level schemes of the isotones ^{96}Sr and ^{98}Zr are shown in Fig. 2.

The 0_3^+ energy in ^{98}Zr is 0.6 keV lower than as given in Ref. [18]. In fact, the evaluator quotes an energy of 213.9 keV for its decay to the 2^+ state. However, former [2] and present measurements yield 213.1(1) keV. After this correction, the quality of the energy fit can be regarded as a justification for placing both $E0$ transitions in cascade between the 0_4^+ and 0_2^+ levels.

The lifetimes of the 0^+ states [2], quoted in Ref. [18], have been recently remeasured by improved techniques [3]. Using the standard procedure [19], we obtain the partial half-lives for the $E0$ transitions given in Table I. The revised ρ^2 values are very large. In particular the value 0.075(8) for the $0_3^+ \rightarrow 0_2^+$ transition is close to the value 0.092(17) for the $0_2^+ \rightarrow 0_1^+$ transition in ^{100}Zr. The upper limits of the intensity of the unobserved, competing $E0$ transitions do not lower this value by more than 3%. Such a large ρ^2 value can only be accounted for by large mixing between the initial and final levels and the presence of sizable deformation. This strongly suggests that the 0_3^+ state at 1436.2 keV can be described as having a major deformed component. The g.s. deformation

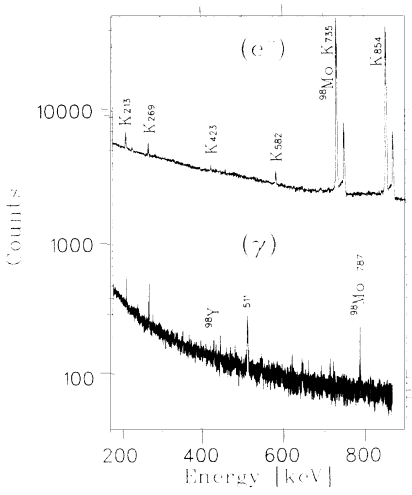

FIG. 1. Electron and γ-ray spectra of the $A = 98$ mass observed at IGISOL. The energy axis has been shifted by the K-electron binding energy of Zr in order to facilitate comparison.

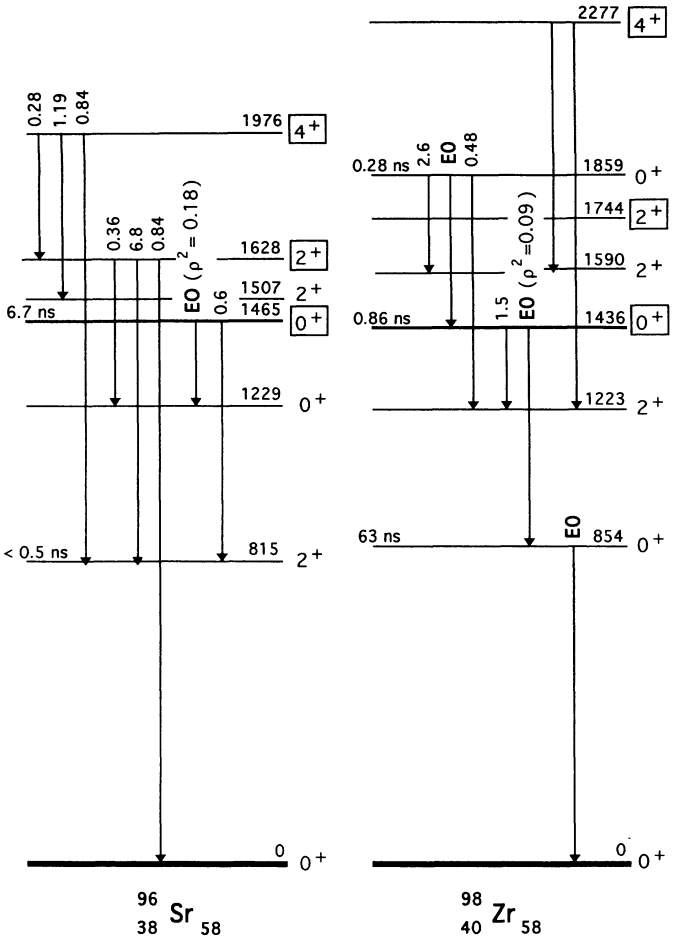

FIG. 2. Partial level schemes of the isotones ^{96}Sr [28] and ^{98}Zr [18,29] showing the proposed deformed bands built on the 0_3^+ states.

of ^{100}Zr is $\beta = 0.36$ [7,8]. If the mixing amplitudes in ^{98}Zr and ^{100}Zr were the same, the deformation of the 1436.2 keV level would amount to $\beta \simeq 0.32$. However, because of the larger $E0$ energy in ^{98}Zr, the mixing is probably less and the deformation might be even larger.

B. The level scheme of ^{99}Zr

The scheme shown in Figs. 3 and 4 is essentially based on coincidence measurements. Gates were set on all previously reported transitions. The new weak transitions could not be used as gating transitions because of the intense background of the precursor activities. Particular care was taken of the γ-ray energy range below 600 keV, which plays a crucial role in revealing weak branchings unobserved so far.

Due to the moderate efficiency at high energy in the OSTIS experiments and the complexity of the singles spectra, some high-energy transitions with less than about 5% relative intensity units are possibly still missing. Energies and intensities determined in the different experiments mostly agree very well; hence we have adopted the averages. The only clear discrepancy concerns the intensity of the 53.3 keV line, which at IGISOL is about 2/3 times weaker than at the other facilities. The IGISOL value is adopted since the efficiency calibration at IGISOL is regarded as the most reliable. The γ rays are listed in Table II and the levels in Table III. New γ rays and levels are included in the level scheme if supported by at least one strong coincidence or two weak but consistent coincidences.

The level scheme for ^{99}Zr has been extended well over the previous version by the group at the JOSEF separator [13]. Almost all new transitions are weak, with intensities typically about 1% of the most intense 121.7 keV transition. The only modifications of the old scheme are the resolving of the doublets at 194 and 930 keV and the new placement of the 639.6 keV transition. The complex peak at 194 keV is resolved into 192.6 and 194.3 keV lines. Both feed the same 657.8 keV level. The 192.6 keV transition deexcites the new level at 850.4 keV, the existence of which is also supported by its feeding by the 865.7 keV transition. The doublet at 930 keV is resolved into a 929.8 keV transition, in agreement with [13], and into a 929.3 keV transition from the new level at 1051.0 keV. The 639.6 keV transition was placed previously elsewhere due to a coincidence with the 536 keV transition which we cannot confirm. We assume that it originates from the 638.7 – 535.7 keV coincidence in the ^{100}Mo scheme [20], which is strongly populated through the decay of ^{100}Nb, a major contaminant in the beam of JOSEF. The 639.6 keV transition deexcites a new level at 761.5 keV.

TABLE I. Data on 0_3^+ and 0_4^+ states in ^{98}Zr. Energies are given in keV, intensities are relative using the normalization of [18].

Level	0_3^+	0_4^+
Energy	1436.1	1859.0
$E2$ energy / intensity	213.1 / 12	268.6 / 21
		636.2 / 4
$E0$ energy / intensity	582.0 / 0.77	423.0 / 0.27
$I(E0)/I(E2)$	0.065 (4)	0.0130 (16)[a]
$t_{1/2}$[b]	0.86 (4)	0.28 (2)
ρ^2_{32}, ρ^2_{43}	0.075 (8)	0.056 (12)
ρ^2_{32}, ρ^2_{43}[c]	0.084 (46)	0.084 (87)
Others	$\rho^2_{31} < 0.015$	$\rho^2_{41} < 0.010$
	$\rho^2_{42} < 0.028$	$\rho^2_{21} = 0.012$ (1)[c]

[a]The ratio is relative to the 269 keV γ transition.
[b]Lifetimes of the 0^+ states [3] are given in ns.
[c]Previous ρ^2 values from [2].

The low-lying levels in ^{99}Zr show a striking similarity to those in its isotone ^{97}Sr [9]. Consequently, the Zr ground state is assumed to be $I^\pi=1/2^+$, while the 121.7 keV level is $3/2^+$ and the 251.9 keV level is $7/2^+$. Since the ^{99}Y ground state is $5/2^+$ [21], we assume the β ground-state branch to be negligible. The deduced log ft values to the excited states are mostly consistent with allowed or first-forbidden β transitions. This renders a determination even of the level parities difficult. In a few cases only, namely for those levels which decay to both $1/2^+$ and $7/2^+$ states, even parity can be established from the γ-decay branchings. Assignments based on the selection rules are shown in Figs. 3 and 4.

Among the new findings, the even parity for the 724.3 keV level and the existence of a cascade with the 87.6 – 53.3 – 614.2 keV transitions are the most important for the discussion of the level stucture of ^{99}Zr. The γ feeding into the 724.3 keV level is weak. Figure 5 shows the low-energy part of a projection gated by this line. The new line at 127.9 keV deexcites the level at 851.9 keV, which has the second strongest β-decay branch (log ft = 6.0). The new line at 87.6 keV is placed from a new

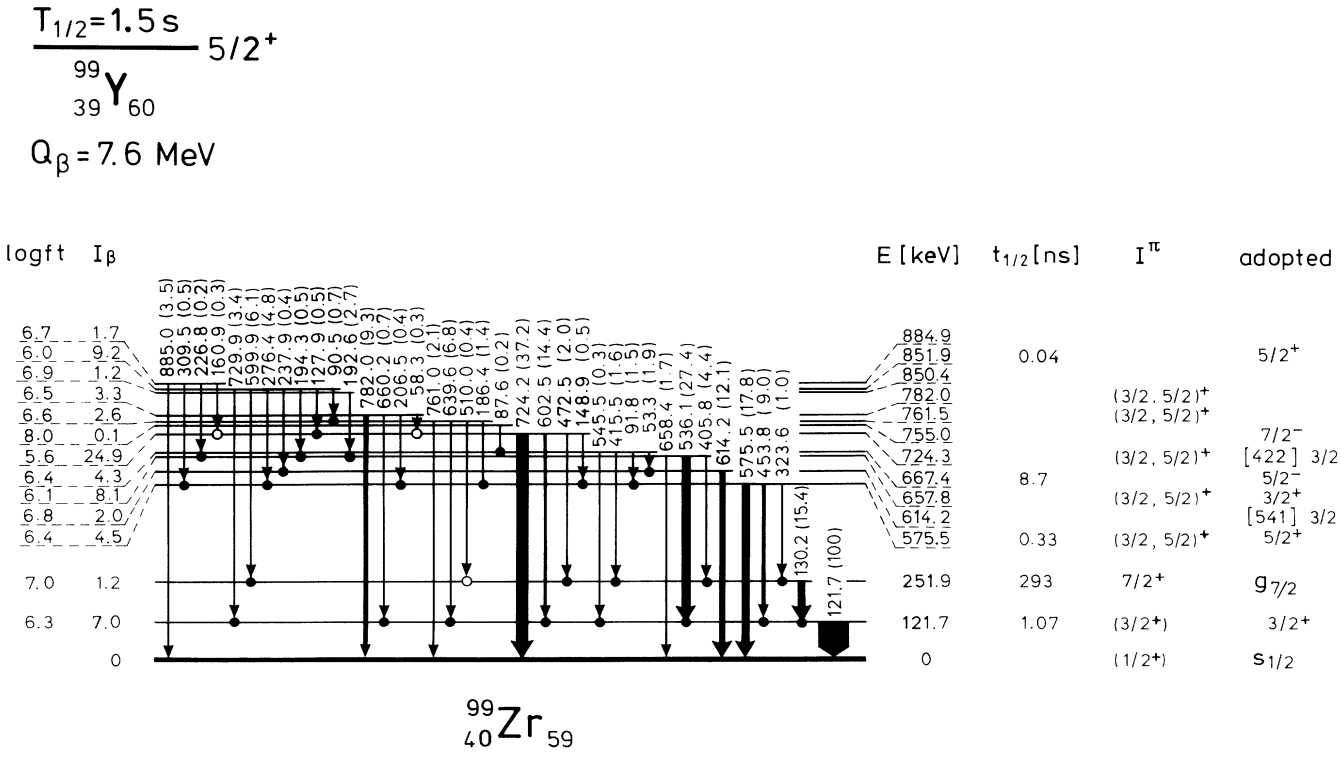

FIG. 3. Lower part of the level scheme of ^{99}Zr as populated in ^{99}Y decay. Adopted spin and parity assignments are discussed in the text.

level at 755.0 keV to the 667.4 keV level, owing to its coincidences with the 614 and 53 keV lines, see Fig. 6. Values of log ft for the levels at 614.2 and 667.4 keV are strongly influenced by the conversion of the 53.3 keV line, which was measured to be $\alpha_K(53) = 2.0(6)$ [22]. Nevertheless, the new weak transitions from the level at 667.4 keV show that this level has a decay pattern in striking correspondence with the level at 713.8 keV in ^{97}Sr [9]. This suggests $I^\pi = 3/2^-$ and $5/2^-$ for the levels at 614.2 and 667.4 keV, respectively. Relative reduced transition probabilities for the $5/2^-$ levels in the isotones ^{97}Sr and ^{99}Zr are shown in Table IV.

IV. THE DEFORMED INTRUDER STATES IN ^{96}Sr AND ^{98}Zr

In analogy to the doubly closed nucleus $^{96}Zr_{56}$, the low-lying states in ^{98}Zr are probably dominated by proton excitations, i.e., promoting a pair of $p_{1/2}$ protons into the $g_{9/2}$ shell [23]. However, in ^{98}Zr two valence neutrons can occupy the $s_{1/2}$ or $g_{7/2}$ orbitals. Thus, going from ^{96}Zr to ^{98}Zr, the increased proton-neutron interaction could be responsible for lowering the 2^+ state from 1751 to 1223 keV and the 0_2^+ state from 1582 to 854 keV. For the

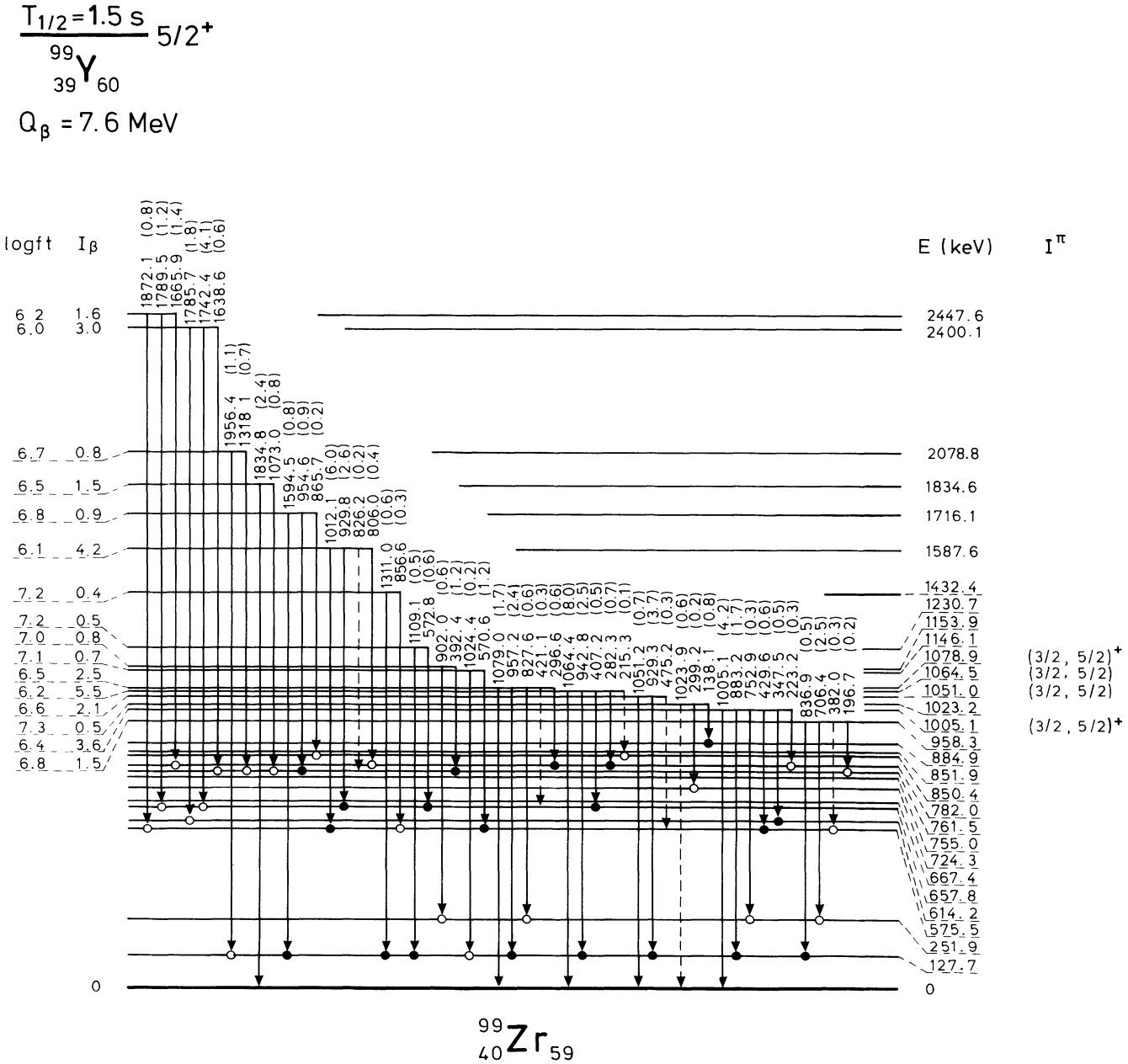

FIG. 4. Upper part of the level scheme of ^{99}Zr as populated in ^{99}Y decay. Adopted spin and parity assignments are discussed in the text.

TABLE II. List of γ rays assigned to the level scheme of ^{99}Zr as populated in the β decay of ^{99}Y. Most of the transitions are assigned and placed from coincidence data. Coincident lines listed are gates in which the γ ray is seen. Weak coincidences are indicated by brackets. The subscript d indicates a gate with a delayed time window on the side of the prompt peak.

Energy (keV)		Intensity		From / to		Coincident lines
53.3	(2)	1.9	(4)	667 /	614	614[a,b]
58.3	(10)	0.3	(3)	782 /	724	(724)[c]
82.8	(10)	0.3	(1)			(576)[d]
87.6	(3)	0.2	(1)	755 /	667	53, (614)
90.5	(2)	0.7	(2)	852 /	761	122, 640
91.8	(2)	1.5	(4)	667 /	576	454, 576
94.2	(3)	0.2	(1)			(122)[e]
115.6	(5)	0.5	(3)			(91)[f]
121.7	(1)	100.0		122 /	0	91, 130, 192, 194, 276, 454, 536, 640, 930, 1012 1742[a,b]
127.9	(3)	0.5	(1)	852 /	724	724
130.2	(1)	15.4	(12)	252 /	122	122[a,b]
138.1	(3)	0.8	(4)	1023 /	885	(160), 724
139.3	(4)	0.3	(1)			(130_d)
141.9	(4)	0.2	(1)			(130_d)
148.9	(2)	0.5	(1)	724 /	576	122, 454, 576
160.9	(8)	0.3	(2)	885 /	724	(724)
185.6	(3)	0.2	(1)			(122_d, (130_d)
186.4	(4)	1.4	(3)	761 /	576	(122), 454, 576
189.1	(3)	0.2	(1)			(122_d), (130_d), (536)[g]
192.6	(2)	2.7	(4)	850 /	658	122, 130_d, 536[b]
194.3	(2)	3.8	(5)	852 /	658	122, 130_d, 536[a,b]
196.7	(3)	0.2	(1)	958 /	761	(640)
206.5	(4)	0.4	(2)	782 /	576	(454), (576)
207.4	(6)	2.6	(13)			(91)[f], (276)[k]
211.1	(6)	0.3	(2)			(130_d)
215.3	(4)	0.1	(1)	1064 /	850	(122), (192), (536)[c]
215.8	(5)	0.5	(2)	791 /	576	(454), (576)[c]
223.2	(4)	0.3	(1)	1005 /	782	(782)
226.8	(4)	0.2	(1)	885 /	658	(130_d), (536)
230.7	(4)	0.2	(1)			(130_d)
237.9	(3)	0.4	(2)	852 /	614	614
276.4	(2)	4.8	(7)	852 /	576	122, 454, 576[a,b]
282.3	(3)	0.7	(2)	1064 /	782	(536), 782
296.6	(3)	0.6	(2)	1079 /	782	782
299.2	(5)	0.2	(1)	1023 /	724	(724)
309.5	(3)	0.5	(2)	885 /	576	(122), 454, 576
315.1	(4)	0.7	(3)	973 /	658	(536)[c]
323.6	(2)	1.0	(3)	576 /	252	130_d
328.5	(5)	0.3	(2)			(724)
347.5	(3)	0.5	(2)	1005 /	658	122, 536
382.0	(5)	0.3	(1)	958 /	576	(576)[d]
392.4	(2)	1.2	(3)	1154 /	761	122, 640[b]
397.6	(3)	0.2	(1)			(122)
405.8	(3)	4.4	(7)	658 /	252	(122), 130_d, (192), 194, (930)[a]
407.2	(4)	0.5	(2)	1064 /	658	(122), (536)
415.5	(2)	1.6	(3)	667 /	252	(130_d)[a,b,h]
421.1	(3)	0.3	(1)	1079 /	658	(122[c])
426.6	(5)	0.7	(2)			(122_d), (130_d)
429.6	(3)	0.6	(2)	1005 /	576	(454), 576
453.8	(2)	9.0	(9)	576 /	122	91, 122, 276, 1012[a,b]
472.5	(2)	2.0	(4)	724 /	252	130_d[a]
475.2	(3)	0.3	(1)	1051 /	576	(122)[c]
510.0	(5)	0.4	(2)	761 /	252	(130_d)
511.1	(3)	0.5	(2)			(576)[d]
527.3	(3)	0.7	(3)			(130_d)
536.1	(3)	27.4	(59)	658 /	122	122, 192, 194, 930, 1742[a,b,i]

TABLE II. (*Continued*).

Energy (keV)		Intensity		From / to		Coincident lines
545.5	(3)	0.3	(1)	667 /	122	122
570.6	(2)	1.2	(2)	1146 /	576	454, 576
572.8	(4)	0.6	(2)	1231 /	658	(122), (536)[j]
575.5	(2)	17.8	(23)	576 /	0	91, 276, 1012[a,b]
599.9	(2)	6.1	(9)	852 /	252	130_d[a,b]
602.5	(2)	14.4	(14)	724 /	122	122[a,b]
614.2	(2)	12.1	(12)	614 /	0	53[a,b]
639.6	(2)	6.8	(8)	761 /	122	91, 122[a]
658.4	(7)	1.7	(5)	658 /	0	(192), (194), (930)
660.2	(3)	0.7	(2)	782 /	122	122
702.9	(3)	0.4	(2)			(930)
706.4	(3)	2.5	(4)	958 /	252	(130_d)
721.6	(3)	0.9	(3)	973 /	252	(130_d)[c]
724.2	(2)	37.2	(44)	724 /	0	[a]
729.9	(2)	3.4	(5)	852 /	122	122[a,b]
752.9	(7)	0.3	(2)	1005 /	252	(130_d)
761.0	(3)	2.1	(4)	761 /	0	(91)
782.0	(2)	9.3	(8)	782 /	0	[a]
806.0	(5)	0.4	(3)	1588 /	782	(782)
826.2	(6)	0.2	(1)	1588 /	761	(122), (122_d)[c]
827.6	(5)	0.6	(3)	1079 /	252	(130_d)
836.9	(4)	0.5	(2)	958 /	122	122
845.7	(6)	0.3	(1)			(122)
856.6	(4)	0.3	(2)	1432 /	576	122, (576)
865.7	(4)	0.2	(1)	1716 /	850	122, (192), (536)
883.2	(3)	1.7	(3)	1005 /	122	122
885.0	(3)	3.5	(12)	885 /	0	
902.0	(5)	0.6	(3)	1154 /	252	(130_d)
929.3	(3)	3.7	(11)	1051 /	122	122
929.8	(3)	2.6	(5)	1588 /	658	122, (130_d), 536[a]
942.8	(2)	2.5	(4)	1064 /	122	122[b]
954.6	(4)	0.9	(3)	1716 /	761	(122), (640)
957.2	(3)	2.4	(4)	1079 /	122	122
1005.1	(3)	4.2	(5)	1005 /	0	
1012.1	(2)	6.0	(11)	1588 /	576	122, 454, 576[a,b]
1023.9	(4)	0.6	(4)	1024 /	0	[c]
1024.4	(6)	0.2	(1)	1146 /	122	(122)
1051.2	(6)	0.7	(3)	1051 /	0	
1064.4	(3)	8.0	(9)	1064 /	0	
1073.0	(4)	0.8	(3)	1835 /	761	122, (640)
1079.0	(4)	1.7	(4)	1079 /	0	
1109.1	(4)	0.5	(2)	1231 /	122	122
1311.0	(4)	0.6	(2)	1432 /	122	122
1318.1	(8)	0.7	(4)	2079 /	761	(640)
1359.6	(7)	0.4	(2)			(122)
1463.1	(6)	0.7	(3)			(122)
1504.2	(7)	0.4	(2)			(122)
1543.7	(7)	0.5	(2)			(122)
1594.5	(5)	0.8	(2)	1716 /	122	122
1638.6	(7)	0.6	(4)	2400 /	761	(640)
1665.9	(6)	1.4	(6)	2448 /	782	(782)[b]
1691.2	(8)	0.4	(2)			(122)
1742.4	(5)	4.1	(8)	2400 /	658	122, (536)[j]
1785.7	(8)	1.8	(7)	2400 /	614	(614)

TABLE II. (*Continued*).

Energy (keV)		Intensity		From / to		Coincident lines
1789.5	(6)	1.2	(4)	2448 /	658	122, (130_d), (536)
1834.8	(6)	2.4	(7)	1835 /	0	
1860.6	(11)	0.6	(3)			(122)
1872.1	(5)	0.8	(5)	2448 /	576	(576)[d]
1956.4	(8)	1.1	(3)	2079 /	122	(122)
1973.1	(8)	0.7	(3)			(122)
1997.5	(9)	0.6	(3)			(122)

[a]Transition observed previously at the separator JOSEF [13].
[b]Transition observed also in singles.
[c]Uncertain transition or placement.
[d]Coincidence could be due to ^{99}Nb.
[e]Possible crosstalk coincidence of 216 keV.
[f]Coincidence could be due to ^{99}Sr.
[g]Possible crosstalk coincidence of 724 keV.
[h]Line contaminated by ^{99}Nb in singles.
[i]Coincidence 122–536 keV from ^{99}Y was subtracted.
[j]Coincidence could be due to ^{99}Y.
[k]Intensity calculated if 207 keV line is on top of 276 keV γ ray.

TABLE III. Levels of ^{99}Zr. Log ft values are calculated using $T_{1/2}(^{99}\mathrm{Y})$= 1.5 s and Q_β= 7.61 MeV [13]. 100 relative γ-intensity units correspond to 47% β feeding from ^{99}Y. Level half-lives are from [13,31].

Energy (keV)		β feeding		log ft	$t_{1/2}$ (ns)
0.		0.0			
121.70	(10)	7.0	(29)	6.3	1.07 (3)
251.90	(14)	1.2	(9)	7.1	293 (10)
575.50	(13)	4.5	(13)	6.4	0.33(2)
614.20	(20)	2.0	(11)	6.8	
657.81	(22)	8.1	(27)	6.1	
667.36	(13)	4.3	(9)	6.4	8.7(5)
724.29	(11)	24.9	(21)	5.6	
754.96	(33)	0.1	(1)	8.0	
761.48	(18)	2.6	(6)	6.6	
781.98	(16)	3.3	(5)	6.5	
850.41	(30)	1.2	(2)	6.9	
851.90	(10)	9.2	(8)	6.0	0.044(11)
884.94	(19)	1.7	(6)	6.7	
958.33	(21)	1.5	(2)	6.8	
1005.09	(15)	3.6	(4)	6.4	
1023.19	(29)	0.5	(2)	7.3	
1051.04	(28)	2.1	(5)	6.6	
1064.49	(15)	5.5	(6)	6.2	
1078.90	(19)	2.5	(3)	6.5	
1146.10	(22)	0.7	(1)	7.1	
1153.89	(24)	0.8	(2)	7.0	
1230.72	(31)	0.5	(1)	7.2	
1432.41	(30)	0.4	(1)	7.2	
1587.61	(20)	4.2	(6)	6.1	
1716.13	(28)	0.9	(2)	6.8	
1834.59	(35)	1.5	(4)	6.5	
2078.83	(74)	0.8	(2)	6.7	
2400.11	(39)	3.0	(6)	6.0	
2447.60	(34)	1.6	(4)	6.2	

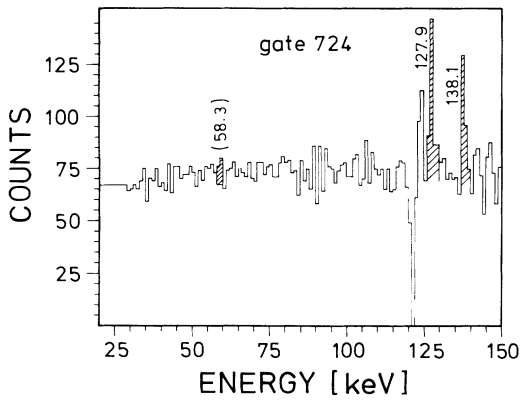

FIG. 5. Projected γ-ray spectrum in coincidence with the 724 keV transition in ^{99}Zr. Hatched transitions are placed in the scheme.

isotone of ^{98}Zr, $^{96}Sr_{58}$, a ρ^2 value of about 0.18 has been reported for the $E0$ decay of the 0_3^+ state at 1465 keV [2]. Thus, the 0_3^+ states in ^{96}Sr and ^{98}Zr lie at the close energies of 1465 keV and 1436 keV, respectively, and both decay by $E0$ transitions with very large ρ^2 values. This suggests the same origin for the 0_3^+ states in Sr and Zr, differing from that of the 0_2^+ states.

Since the mixing amplitudes are unknown, deformations cannot be extracted from the ρ^2 values. However, it would be very interesting to have an estimate of the deformation of the intruder states in ^{96}Sr and ^{98}Zr in order to see how they compare with deformations measured at larger neutron number. The ground-state deformations of the Sr isotopes are well known, owing to extensive measurements by lifetime techniques [1,4,5,24] and by laser spectroscopy [25,26]. The deformations, from the lifetimes of the 2^+ states, of the ground-state bands of the Zr isotopes with $N \geq 60$ are also well established [7,8]. We estimate the deformations in ^{96}Sr and ^{98}Zr from a plot of the static moment of inertia versus deformation. For even-even nuclei ranging from ^{98}Sr to ^{104}Mo a linear correlation is well established [27] and it has been related to the observation of identical ground-state bands in ^{98}Sr and ^{100}Sr.

Sets of levels in both ^{96}Sr and ^{98}Zr form reasonable candidates for the bands built on the 0_3^+ states. In ^{96}Sr the levels at 1975.7 (possibly 4^+) and at 1628.2 keV (2^+) form a level sequence with an $E(4^+)/E(2^+)$ ratio of 3.1, characteristic of a good rotor. The deformation derived from the correlation plot [27], $\beta = 0.35$, compares very well with the value of 0.40 for the $N \geq 60$ Sr isotopes. In ^{98}Zr also, a band built on the deformed 0^+ state at 1436 keV can be postulated. The proposed next members are the 2^+ level at 1744.3 keV and the 4^+ level [29] at 2276.6 keV, yielding $E(4^+)/E(2^+)$=2.7. The poorer agreement with the rigid-rotor value might be a consequence of the interaction of the 2^+ level with another 2^+ state at 1590.5 keV. The deduced deformation of $\beta = 0.25$ is near the limit extracted from the ρ^2 value at maximal mixing. The only alternative, with band members at 1590.5 (2^+) and 2047.6 keV (4^+), would result in a moment of inertia which exceeds the largest ones in the deformed region.

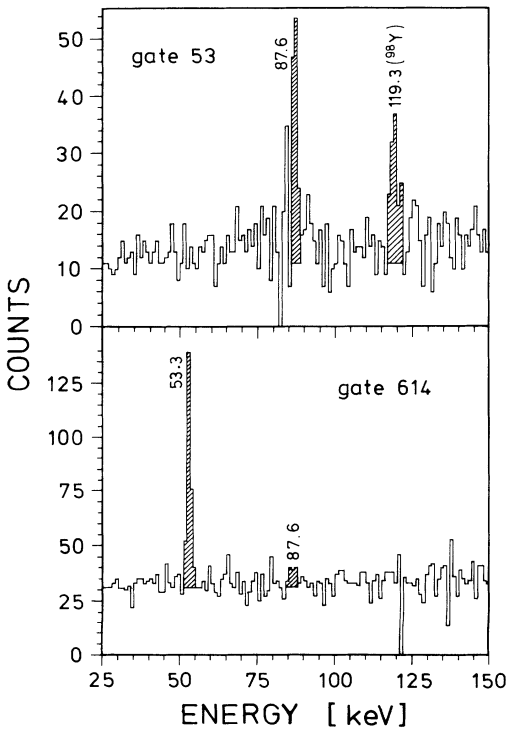

FIG. 6. Projected γ-ray spectra in coincidence with the 53 keV and 614 keV transitions in ^{99}Zr, showing the low-energy interband transitions.

V. STRUCTURE OF ^{99}Zr

A comparison of the level properties, in particular of the relative reduced transition probabilities, in $^{99}Zr_{59}$ and in $^{97}Sr_{59}$ [9] is the key for understanding the structure of ^{99}Zr. At low excitation energy ^{97}Sr is spherical and the $s_{1/2}$ and $g_{7/2}$ neutron shells determine the low-lying level structure. The $1/2^+$ ground state and the second excited $7/2^+$ state are thus assigned to these orbitals. The first excited state $I^\pi=3/2^+$ has a more complex structure, which involves admixtures of the $2^+ \otimes g_{7/2}$ coupling and the $d_{3/2}$ single-particle level. These level energies and transition probabilities have been well reproduced in the framework of the interacting boson fermion (IBF) model [9]. Because of the striking similarity of the low-lying levels in ^{97}Sr and ^{99}Zr [13], there is hardly a doubt that ^{99}Zr is spherical at low excitation energy and in its ground state. Thus, the levels at 121.7 and 251.9 keV are assigned $1/2^+$, $3/2^+$, and $7/2^+$, respectively. The similarity between ^{97}Sr and ^{99}Zr is further obvious from the general features of their level schemes. Above these levels, after an energy gap of about 300 keV, the level density increases, and still β-feeding strengths and γ-decay patterns look very similar. From its γ branchings the $(3/2, 5/2)^+$ level at 575.5 keV seems to correspond to the level at 600.5 keV in ^{97}Sr. The latter was assigned $I^\pi=5/2^+$ [30] and the $2^+ \otimes s_{1/2}$ configuration was later proposed by Büscher *et al.* [11]. New half-life measurements on ^{99}Zr [31] yield 0.6 single-particle units

TABLE IV. Comparison between the γ-decay branchings of the $5/2^-$ states in ^{97}Sr and ^{99}Zr. Quoted are the relative reduced branching ratios (after removing the E_γ^3 dependence), normalized to 100. The $E2$ admixtures in the proposed intraband transitions to the $3/2^-$ bandheads have been neglected. The δ^2 values are about 0.03 in ^{97}Sr [9] and 0.17(14) in ^{99}Zr [22].

	^{97}Sr		^{99}Zr		Proposed final level
	E_{level}	$B(\lambda=1)$	E_{level}	$B(\lambda=1)$	configuration
$E(5/2^-)$ (keV)	714		667		
$\log ft$		6.2		6.4	
$B(E1,\rightarrow 3/2_1^+)$	167	0.01	122	0.01	
$B(E1,\rightarrow 7/2_1^+)$	308	0.04	252	0.06	$g_{7/2}$
$B(E1,\rightarrow 3/2_2^+)$	585	4	724		[422]3/2
$B(E1,\rightarrow 5/2_1^+)$	601	3	576	5	$(2^+ \otimes s_{1/2})_{5/2}$
$B(E1,\rightarrow (3/2,5/2)^+$	522		658		$(2^+ \otimes s_{1/2})_{3/2}$
$B(M1,\rightarrow 3/2^-)$	645	93	614	95	[541]3/2

($E2$) for the g.s. transition if $I^\pi=5/2^+$ is assumed for the 575.5 keV level. Thus this interpretation seems reasonable. The 657.8 keV level could correspond to the 522.4 keV one in ^{97}Sr since both have their strongest decay branch to the first excited $3/2^+$ state. These levels are candidates for the $3/2^+$ level expected from the $2^+ \otimes s_{1/2}$ coupling.

The levels at 614.2 and 667.4 keV are connected by the 53.3 keV transition with a strong $E2$ component [22]. From a calculation using the rotor + particle model Liang *et al.* [31] concluded that these levels are deformed and assigned the band head at 614.2 keV to the [422]$3/2^+$ orbital. We note, however, that in ^{97}Sr the $\log ft$ value for the β decay to the [422]3/2 state is 5.6 and such a low value is clearly excluded for the 614.2 keV level in ^{99}Zr. There is no obvious reason why this β decay should be ten times more hindered in Zr than in Sr. However, we already noticed the exceptionally close correspondence between the decay patterns of the 667.4 keV level and of the 713.8 keV level in ^{97}Sr (Table IV), and assigned $5/2^-$ to the 667.4 keV level. Accordingly, the 614.2 keV level is assigned $3/2^-$ and it is proposed as the head of a band built on the [541]3/2 Nilsson orbital. The 667.4 keV level is thus the next $I^\pi=5/2^-$ band member. The new level at 755.0 keV, which decays only to the $5/2^-$ state, is a candidate for the $7/2^-$ level. As in ^{97}Sr, this band is strongly compressed, see Fig. 7. The $5/2 \rightarrow 3/2$ energies of 69.1 (^{97}Sr) and 53.3 keV (^{99}Zr) are much lower than the values of about 90 keV for the [411]3/2 band [17] in the strongly deformed region. This is likely a result of Coriolis mixing, since the [541]3/2 orbital is a low-K orbital of high-j parentage ($h_{11/2}$). In a recent experiment on prompt fission [32], it was shown that the low-spin members of these bands are indeed perturbed.

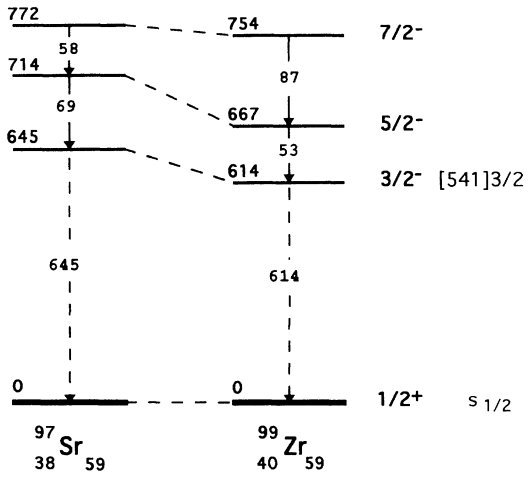

FIG. 7. Comparison of the $3/2^-$ bands in the isotones ^{97}Sr [9] and ^{99}Zr.

The level at 724.3 keV is remarkable by the strength of its β feeding, with $\log ft$=5.6. It is tempting to attribute this feeding to a Gamow-Teller transition. Since the structure of the parent nucleus ^{99}Y is dominated by the [422]5/2 proton orbital [21], the 724.3 keV level must be associated with the [422]3/2 neutron orbital and corresponds to the 585.1 keV level in ^{97}Sr [9,11]. The 851.9 keV level is the best candidate, if any, for the next $5/2^+$ band member. It decays, among other branches, to the level at 724.3 keV through a 127.9 keV γ ray. Its partial half-life, using the level half-life of 44(11) ps [31] is 1.7 ns, while the pure $M1$ and $E2$ single-particle values are 0.01 and 598 ns, respectively. Thus, reasonable hindrance of the $M1$ and enhancement of the $E2$ component are consistent with the experimental half-life. We may summarize this part as follows: Although well-developed band structures have not been observed, there is good evidence for the existence of deformed states near 600 keV excitation energy in ^{99}Zr.

VI. DISCUSSION

The deformation of the 0_3^+ state in ^{98}Zr has been firmly established, and strong evidence exists for a deformation of the 0_3^+ state in ^{96}Sr, too. In contrast to the strong increase of the excitation energies of the 2^+ and 0_2^+ states from $_{38}$Sr to $_{40}$Zr, the excitation energy of the 0_3^+ states, 1464.6 keV in ^{96}Sr and 1436.2 keV in ^{98}Zr, respectively, shows a remarkably small variation with proton number. The deformed 0_3^+ states in the $N=58$ isotones ^{96}Sr and ^{98}Zr must correspond to the strongly deformed ground

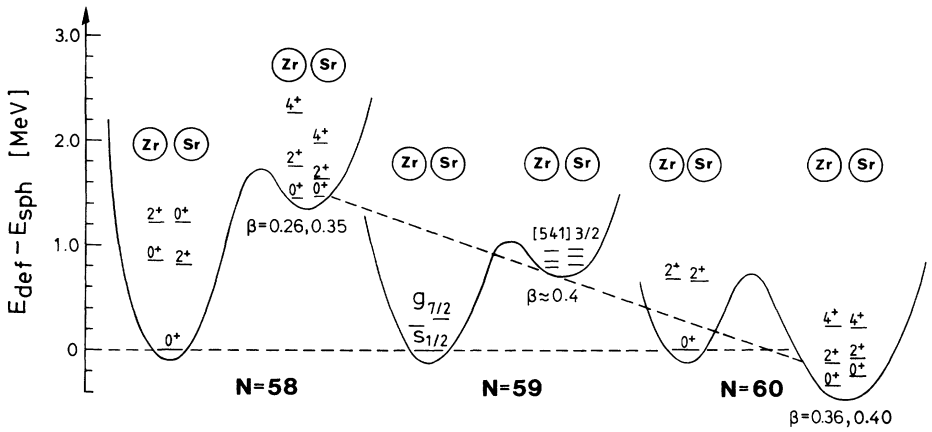

FIG. 8. Systematics of deformed states in the even-even Sr and Zr nuclei with $N = 58$ [18,28,29] and $N = 60$ [4,7,8]. The lowest deformed states in the intermediate odd-neutron isotones ^{97}Sr [9] and ^{99}Zr are also shown. The position of the lowest spherical states has been adjusted. Dashed lines connecting the minima of the potential wells and the solid lines showing their shape are only a guide to the eye.

states in the $N = 60$ isotones ^{98}Sr and ^{100}Zr, respectively. The ρ^2 values are close to each other and the estimates of deformation for the excited states in the $N = 58$ isotones compare well with the ones measured for the ground states of the $N = 60$ isotones.

Moreover, in ^{99}Zr there is good evidence for deformation in excited states, and this implies that the intermediate $N = 59$ isotones ^{97}Sr, ^{98}Y, and ^{99}Zr all have a deformed minimum near 600 keV excitation energy. In the odd-neutron isotones ^{97}Sr and ^{99}Zr, the lowest deformed states lie close in energy, too. The [541]3/2 orbital is at 644.7 keV in ^{97}Sr and at 614.2 keV in ^{99}Zr above the respective $s_{1/2}$ spherical ground states. The [422]3/2 orbital is at 585.1 keV in ^{97}Sr, and we associate it with the 724.3 keV level in ^{99}Zr. The higher energy of the $3/2^+$ bandhead in ^{99}Zr can be understood using the Nilsson scheme (see, e.g., Fig. 4 in Ref. [5]). The Fermi level at $N = 59$ is close to the strongly down-sloping [541]3/2 orbital. This orbital crosses the [422]3/2 orbital, which is less steep versus deformation. At the large deformation corresponding to ^{97}Sr ($\beta \simeq 0.4$ [11]), the two orbitals lie near each other. For ^{99}Zr, in agreement with the deformations measured for the ground-state bands at $N \geq 60$ and our estimates for the excited bands at $N = 58$, it is reasonable to assume a smaller deformation than for ^{97}Sr. A value of $\beta = 0.40(10)$ is derived in Ref. [22] from the lifetime of the 53.3 keV transition. This value, however, is not very significant since the band is strongly perturbed. With decreasing deformation, the [422]3/2 orbital moves deeper below the Fermi surface and, accordingly, the $3/2^+$ level appears in the level spectrum at a higher energy.

There is a simple trend of the energies of the lowest identified deformed states, when the relevant spherical states are taken as reference (see Fig. 8), for the Sr and Zr isotopes with $N = 58$, 59 and 60. They show little dependence on proton number and they lie almost on a straight line, suggesting that they correspond to the regular lowering of the deformed minimum with increasing neutron number. Thus the sudden drop in the 2^+ energies of the Sr and Zr isotopes from $N = 58$ to $N = 60$ turns out to result from the comparison of levels in spherical and deformed potential wells. The change is so rapid because the spherical nuclei are situated at strong subshell closures, pushing the energy upwards, whereas the deformed ones show unusually large deformations and large moments of inertia, corresponding to especially low energies.

In contrast to this simple interpretation, the sudden onset of deformation has been explained by invoking a strong proton-neutron interaction. For the $^{96-98}$Zr isotopes the intruding 0_2^+ states are interpreted as proton excitations across the $p_{1/2}$-$g_{9/2}$ subshell gap [23]. Under the influence of the strong proton-neutron interaction between the spin-orbit partner orbitals $\pi g_{9/2}$-$\nu g_{7/2}$, the addition of a neutron pair to the $g_{7/2}$ orbital will eradicate the gap and create the large valence space necessary for the onset of deformation. Shell-model calculations in that spirit have also been reported [33]. However, this effect is not visible in the calculations of Kumar and Gunye using a much larger model space [34].

The qualitative features of the shape transition in this region are well reproduced by a pairing + quadrupole model, showing the importance of the p-n interaction [35]. The present measurements provide a simple explanation for the sudden onset of deformation in the $A \simeq 100$ region. The mechanism of an extra strong p-n interaction acting on the 0_2^+ states need not be invoked. The p-n interaction needs to be responsible only for the (still very rapid) lowering of the deformed minimum. As a matter of fact, not only the interaction between the spin-orbit partners $\pi g_{9/2}$-$\nu g_{7/2}$ but also between the $\pi g_{9/2}$-$\nu h_{11/2}$ orbits seems to be important in this region [5].

ACKNOWLEDGMENTS

This work was supported by the German Federal Ministery for Research under Contract No. 06 MZ 106 and the Academy of Finland. One of the authors (G.L.) would like to thank Professor K. Sistemich for helpful discussions.

[1] H. Mach, F. K. Wohn, G. Molnar, K. Sistemich, J. C. Hill, M. Moszynski, R. L. Gill, W. Krips, and D. S. Brenner, Nucl. Phys. **A523**, 197 (1991).
[2] K. Kawade, G. Battistuzzi, H. A. Selič, K. Sistemich, F. Schussler, E. Monnand, J. A. Pinston, B. Pfeiffer, and G. Jung, Z. Phys. A **304**, 293 (1982).
[3] H. Mach, R. L.Gill, and M. Moszynski, Nucl. Instrum. Methods A **280**, 49 (1989).
[4] H. Ohm, G. Lhersonneau, K. Sistemich, B. Pfeiffer, and K.-L. Kratz, Z. Phys. A **327**, 483 (1987).
[5] G. Lhersonneau, H. Gabelmann, N. Kaffrell, K.-L. Kratz, B. Pfeiffer, K. Heyde, and the ISOLDE Collaboration, Z. Phys. A **337**, 213 (1990).
[6] F. K. Wohn, H. Mach, M. Moszynski, R. L. Gill, and R. F. Casten, Nucl. Phys. **A507**, 141 (1990).
[7] H. Ohm, M. Liang, G. Molnar, and K. Sistemich, Z. Phys. A **334**, 519 (1989).
[8] H. Mach, M. Moszynski, R. L. Gill, F. K. Wohn, J. A. Winger, J. C. Hill, G. Molnar, and K. Sistemich, Phys. Lett. B **230**, 21 (1989).
[9] G. Lhersonneau, B. Pfeiffer, K.-L. Kratz, H. Ohm, K. Sistemich, S. Brant, and V. Paar, Z. Phys. A **337**, 149 (1990).
[10] H. Mach and R. L. Gill, Phys. Rev. C **36**, 2721 (1988).
[11] M. Büscher, R. F. Casten, R. L. Gill, R. Schumann, J. A. Winger, H. Mach, M. Moszynski, and K. Sistemich, Phys. Rev. C **41**, 1115 (1990).
[12] H. Mach, F. K. Wohn, M. Moszynski, R. L. Gill, and R. F. Casten, Phys. Rev. C **41**, 1141 (1990).
[13] H. W. Mueller and D. Chmielewska, Nucl. Data Sheets **48**, 663 (1986).
[14] P. Taskinen *et al.*, Nucl. Instrum. Methods Phys. Res. A **281**, 539 (1989).
[15] P. P. Jauho, A. Jokinen, M. Leino, J. M. Parmonen, H. Penttipä, J. Äystö, K. Eskola, and V. A. Rubchenya (submitted to Phys. Rev. C).
[16] J. M. Parmonen *et al.*, Nucl. Instrum. Methods Phys. Res. A **306**, 504 (1991).
[17] B. Pfeiffer, E. Monnand, J. A. Pinston, J. Muenzel, P. Moeller, J. Krumlinde, W. Ziegert, and K.-L. Kratz, Z. Phys. A **317**, 123 (1984); B. Pfeiffer, S. Brant, K. L. Kratz, R. A. Meyer, and V. Paar, *ibid.* **325**, 487 (1986).
[18] H. W. Mueller, Nucl. Data Sheets **39**, 467 (1983).
[19] J. Kantele, in *Heavy Ions and Nuclear Structure*, edited by B. Sikora and Z. Wilhelmi (Harwood Academic, London, 1984).
[20] B. Sing and J. A. Szucs, Nucl. Data Sheets **60**, 1 (1990).
[21] R. A. Meyer, E. Monnand, J. A. Pinston, F. Schussler, I. Ragnarson, B. Pfeiffer, H. Lawin, G. Lhersonneau, T. Seo, and K. Sistemich, Nucl. Phys. **A439**, 510 (1985).
[22] K. Kawade, G. Lhersonneau, H. Ohm, K. Sistemich, and R. A. Meyer, KFA-Jülich Report, 1986, p. 21.
[23] K. Heyde, J. Jolie, J. Moreau, J. Ryckebusch, M. Waroquier, P. Van Duppen, M. Huyse, and J. L Wood, Nucl. Phys. **A466**, 189 (1987).
[24] G. Lhersonneau, H. Gabelmann, N. Kaffrell, K.-L. Kratz, B. Pfeiffer, and the ISOLDE Collaboration, Z. Phys. A **332**, 243 (1989).
[25] F. Buchinger, E. B. Ramsay, E. Arnold, W. Neu, R. Neugart, K. Wendt, R. E. Silverans, P. Lievens, L. Vermeeren, D. Berdichevsky, R. Fleming, D. W. L. Sprung, and G. Ulm, Phys. Rev. C **41**, 2883 (1990).
[26] P. Lievens, R. E. Silverans, L. Vermeeren, W. Borchers, W. Neu, R. Neugart, K. Wendt, F. Buchinger, E. Arnold, and the ISOLDE Collaboration, Phys. Lett. B **256**, 141 (1991).
[27] G. Lhersonneau, K.-L. Kratz, J. Äystö, H. Gabelmann, J. Kantele, and B. Pfeiffer, the OSTIS and the ISOLDE Collaborations, Proceedings of the Sixth International Conference on Nuclei Far From Stability and the Ninth International Conference on Atomic Masses and Fundamental Constants, Institute of Physics Conference Series Number 132, edited by R. Neugart and A. Wöhr (IPP, Bristol and Philadelphia, 1992), p. 545.
[28] H. W. Mueller, Nucl. Data Sheets **35**, 281 (1982).
[29] M. L. Stolzenwald, S. Brant, H. Ohm, K. Sistemich, and G. Lhersonneau, *Proceedings of the International Workshop on Nuclear Structure of the Zr region*, Springer Reports on Physics, edited by J. Eberth, R. A. Meyer, and K. Sistemich (Springer-Verlag, Berlin, 1988), p. 239.
[30] K.-L. Kratz, H. Ohm, A. Schroeder, H. Gabelmann, W. Ziegert, B. Pfeiffer, G. Jung, E. Monnand, J. A. Pinston, F. Schussler, G. I. Crawford, S. G. Prussin, and Z. M. de Oliviera, Z. Phys. A **312**, 43 (1983).
[31] M. Liang, H. Ohm, M. Buescher, G. Lhersonneau, and K. Sistemich, KFA-Jülich Report, 1991, p. 81.
[32] M. C. A. Hotchkis, J. L. Durell, J. B. Fitzgerald, A. S. Mowbray, W. R. Phillips, I. Ahmad, M. P. Carpenter, R. V. F. Janssens, T. L. Khoo, E. F. Moore, L. R. Morss, Ph. Benet, and D. Ye, Nucl. Phys. **A530**, 111 (1991).
[33] A. Etchegoyen, P. Federmann, and E. G. Vergini, Phys. Rev. C **39**, 1130 (1989).
[34] A. Kumar and M. R. Gunye, Phys. Rev. C **32**, 2116 (1985).
[35] M. Sugita and A. Arima, Nucl. Phys. **A515**, 77 (1990).